MOLECULAR AND CELLULAR BIOLOGY, Aug. 2000, p. 5619–5630 Vol. 20, No. 15
0270-7306/00/$04.00+0


# Nup50, a Nucleoplasmically Oriented Nucleoporin with a Role in Nuclear Protein Export

TINGLU GUAN,[1] RALPH H. KEHLENBACH,[1] ERIC C. SCHIRMER,[1] ANGELIKA KEHLENBACH,[1] FAN FAN,[2] BRUCE E. CLURMAN,[3] NORMAN ARNHEIM,[2] AND LARRY GERACE[1]*

*Departments of Cell and Molecular Biology, The Scripps Research Institute, La Jolla, California 92037[1]; Molecular Biology Program, University of Southern California, Los Angeles, California 90089-1340[2]; and Clinical Research and Human Biology Divisions, Fred Hutchinson Cancer Research Center, Seattle, Washington 98140[3]*

Received 1 February 2000/Returned for modification 7 March 2000/Accepted 19 April 2000

**We present here a detailed analysis of a rat polypeptide termed Nup50 (formerly NPAP60) that was previously found to be associated with the nuclear pore complex (F. Fan et al., Genomics 40:444–453, 1997). We have found that Nup50 (and/or a related 70-kDa polypeptide) is present in numerous rat cells and tissues. By immunofluorescence microscopy, Nup50 was found to be highly concentrated at the nuclear envelope of rat liver nuclei, whereas in cultured NRK cells it also is abundant in intranuclear regions. On the basis of immunogold electron microscopy of both rat liver nuclear envelopes and NRK cells, we determined that Nup50 is specifically localized in the nucleoplasmic fibrils of the pore complex. Microinjection of anti-Nup50 antibodies into the nucleus of NRK cells resulted in strong inhibition of nuclear export of a protein containing a leucine-rich nuclear export sequence, whereas nuclear import of a protein containing a classical nuclear localization sequence was unaffected. Correspondingly, CRM1, the export receptor for leucine-rich export sequences, directly bound to a fragment of Nup50 in vitro, whereas several other import and export receptors did not significantly interact with this fragment. Taken together, our data indicate that Nup50 has a direct role in nuclear protein export and probably serves as a binding site on the nuclear side of the pore complex for export receptor-cargo complexes.**

Molecular transport between the nucleus and cytoplasm is mediated by nuclear pore complexes (NPCs), large supramolecular structures that span the nuclear envelope (NE) (reviewed in references 9 and 39). Small molecules and proteins (<20 to 40 kDa) can passively diffuse through the NPC, whereas most proteins and RNAs are transported through the NPC by signal- and energy-dependent mechanisms (reviewed in references 1, 17, and 26). In most cases, signal-mediated transport of nuclear proteins is mediated by nucleocytoplasmic shuttling carriers of the importin β/karyopherin β family (reviewed in reference 44). These transport receptors interact with cargo molecules in the originating compartment and then are translocated through the NPC as receptor-cargo complexes prior to cargo dissociation from the receptors and receptor recycling.

In addition to shuttling receptors, several additional cytosolic factors participate in the signal-mediated transport of cargo through the NPC, including the small GTPase Ran, and the Ran-binding proteins NTF2 and RanBP1 (reviewed in references 17, 26, and 27). The GTP-bound form of Ran directly associates with importin β/karyopherin β-related receptors and plays a key role in determining the directionality of transport. Whereas the binding of RanGTP to import receptors promotes cargo dissociation, the binding of RanGTP to export receptors promotes cargo binding (reviewed in references 17, 26, and 27). Since RanGTP is believed to have a high concentration in the nucleus relative to the cytoplasm, Ran is likely to be involved in the loading and unloading of transport receptors in the nucleus. An additional role for RanGTP in vectorial transport through the NPC is suggested by the finding that RanGTP targets export complexes to the cytoplasmic side of the NPC (8, 24).

It is likely that a large number of different signals exist for receptor-mediated nuclear transport, corresponding to the large diversity of importin β/karyopherin β-like receptors that is apparent in yeasts and higher eukaryotes (31, 44). However, only a relatively small number of nuclear transport signals have been characterized in detail (reviewed in references 1, 17, and 26). The classical signal for nuclear protein import (nuclear localization signal [NLS]) is a short segment of amino acids enriched in basic amino acid residues, arranged in either a single or bipartite motif. The classical NLS binds to its cognate receptor, importin β/karyopherin β via the adapter protein importin α/karyopherin α (reviewed in references 1, 17, and 26). The best-characterized nuclear protein export signal is a short amino-acid sequence enriched in leucine residues, which directly binds to the export receptor CRM1 (13, 38). Many of the signals that specify RNA export from the nucleus probably reside on proteins bound to the RNA, although in the case of tRNA the nuclear export signal (NES) that binds to the shuttling transport receptor consists of a segment of the tRNA itself (3, 25).

The NPC (reviewed in references 9 and 39) has an estimated mass of ~125 MDa in vertebrate cells and is somewhat smaller in yeast cells. It consists of nucleoplasmic and cytoplasmic rings flanking eight central spokes (20), which embrace an operationally defined central gated channel that is the site of signal-mediated transport. Extending outward from the nuclear and cytoplasmic rings are flexible fibrils ca. 50 to 100 nm long (23, 34), which may represent initial and terminal binding sites for transport complexes during passage through the NPC. The vertebrate NPC is thought to comprise ca. 50 to 100 different polypeptides (nucleoporins), of which about 20 have been molecularly characterized (39). Among these are a group of polypeptides characterized by multiple copies of FG (phenylala-

* Corresponding author. Mailing address: Departments of Cell and Molecular Biology, The Scripps Research Institute, 10550 N. Torrey Pines Rd., La Jolla, CA 92037. Phone: (858) 784-8514. Fax: (858) 784-9132. E-mail: lgerace@scripps.edu.

nine and glycine) repeats dispersed through a portion of their sequence. Many FG repeat proteins have been found to bind directly to importin β/karyopherin β-like nuclear transport receptors (14, 22, 24, 28, 33, 35), and appear to represent binding sites for transport complexes during their movement through the NPC. In vertebrates, some FG repeat proteins are found on the nucleoplasmic fibrils (Nup153 and Nup98), others are restricted to the cytoplasmic fibrils (Nup214 [Can], Nup358 [RanBP2]), and yet others are found on both sides of the NPC near the central gated channel (the p62 complex, consisting of three or four different FG repeat proteins) (reviewed in reference 39). Recent work has linked specific nucleoporins (or different regions of specific nucleoporins) to different receptor-mediated transport pathways (reviewed in reference 17). Understanding the detailed mechanism of signal-mediated transport through the NPC will require, as a first step, the identification of the specific nucleoporins involved in the movement of different receptor-cargo complexes.

In this study we have analyzed a nuclear pore-associated protein (previously termed NPAP60, herein designated Nup50) that had been previously characterized by cDNA cloning in rat testis (10). This protein has five FG repeat motifs and is more hydrophilic in character than most of the previously described FG repeat nucleoporins. By immunofluorescence microscopy, Nup50 was found to have an NPC-like localization in cultured rat cells and, in spermatogenic cells, to have either an NPC-like or an intranuclear distribution depending on the spermatogenic stage (10). Here we show that this polypeptide is present in a wide range of different rat cells and is localized specifically to the nucleoplasmic fibrils of the NPC. Antibody injection and biochemical approaches indicate that Nup50 has a direct role in CRM1-mediated nuclear protein export. Thus, Nup50 joins a group of several other discrete nucleoporins that have now been implicated in this export pathway.

## MATERIALS AND METHODS

**Production of antibodies against Nup50.** One batch of polyclonal antibodies against Nup50 (antibody 1) (see Results) was obtained as described previously (10) by immunizing rabbits with a recombinant fragment of Nup50 (residues 173 to 357) fused to an oligohistidine tag. Anti-Nup50 antibodies were affinity purified by passing the serum over a column consisting of the immunizing antigen conjugated to CNBr-activated Sepharose 4B beads. After washing the column in phosphate-buffered saline (PBS) containing 500 mM NaCl, the antibodies were eluted from the Nup50 beads with 100 mM glycine (pH 2.7), neutralized with 2 M Tris-HCl (pH 8.8), and dialyzed against PBS. A second batch of antibodies (antibody 2) (see Results) was obtained by immunizing rabbits with His-tagged mouse Nup50 produced in *Escherichia coli* (36a). The antibodies were affinity purified as follows: His-tagged murine Nup50 was electrophoresed on a sodium dodecyl sulfate (SDS) gel, and the protein was transferred to a polyvinylidene difluoride membrane. An excised membrane strip containing the Nup50 band was incubated with anti-Nup50 antiserum, and the bound antibody was eluted with 0.1 M glycine-HCl (pH 2.2), neutralized, and dialyzed against PBS. In some cases, the antibodies were then dialyzed into microinjection buffer (10 mM sodium phosphate, pH 7.2; 80 mM KCl; 5% glycerol).

**Expression and purification of recombinant transport substrates and receptors.** The cDNA encoding the leucine-rich NES substrate, which consists of glutathione *S*-transferase (GST) fused to the NES of PKI (residues 37 to 46 [43]), was provided by Susan Taylor (University of California, San Diego). The cDNA encoding the classical (basic-amino-acid-rich) NLS substrate, which consists of GST fused to a region of lamin A containing its NLS (residues 396 to 430), was obtained as described previously (40). For the production of these proteins in *E. coli*, the cDNAs were transformed into BL21(pLysS) cells and recombinant protein expression was induced by incubation with 2 mM IPTG (isopropyl-β-D-thiogalactopyranoside) for 4 h (40). The fusion proteins were purified by adsorption of the GST fusion proteins from soluble lysates of bacteria to a glutathione-agarose column and elution with glutathione. The eluted proteins were dialyzed into microinjection buffer and stored at −80°C after freezing in liquid nitrogen. The isolated fusion proteins were >95% pure based on Coomassie blue staining of SDS gels.

To obtain recombinant CRM1 and CAS, we used pQE60-CRM1 provided by I. Mattaj (EMBL, Heidelberg, Germany) and pQE30-CAS provided by D. Görlich (ZMBH, Heidelberg, Germany). The plasmids were transformed into TG1 bacteria, and the recombinant proteins were expressed by overnight incubation in Luria-Bertani medium without induction at 37°C. Then, 0.5 mM phenylmethylsulfonyl fluoride (PMSF) was added to the culture prior to centrifugation at 4,000 × *g* for 10 min. The bacterial pellet was resuspended to 2% of the original volume with lysis buffer (50 mM HEPES [pH 8]–500 mM NaCl–2 mM $MgCl_2$ [for CRM1] or 100 mM HEPES [pH 8]–300 mM NaCl–0.5 mM EDTA [for CAS] supplemented with 1 mM PMSF and 5 μg each of aprotinin, leupeptin, and pepstatin per ml) and stored at −80°C prior to lysis by sonification. After centrifugation at 100,000 × *g* for 45 min, saturated ammonium sulfate was added to the supernatant to a final concentration of 1.4 M. The precipitate was collected by centrifugation at 10,000 × *g* for 20 min. The pellet was resuspended to 0.5% of the original volume with wash buffer: 100 mM HEPES (pH 8)–200 mM NaCl–5 mM $MgCl_2$–10% glycerol (for CAS) or 50 mM HEPES (pH 8)–500 mM NaCl–2 mM $MgCl_2$ (for CRM1), both supplemented with 5 mM imidazole, 1 mM PMSF, 20 μg of DNase per ml, and 5 μg each of aprotinin, leupeptin, and pepstatin per ml and then incubated with Talon beads (Clontech Laboratories, Inc., Palo Alto, Calif.) for 1 h at 4°C with gentle agitation. The beads were collected by centrifugation and then washed with wash buffer with 10 mM imidazole. The proteins were eluted with 50 to 100 mM imidazole in the same buffer, and peak fractions were dialyzed against transport buffer. Aliquots were frozen in liquid nitrogen and stored at −80°C.

**Subcellular fractionation and immunoblotting.** Rat liver NEs were isolated as described earlier (16) by digestion of isolated rat liver nuclei with DNase-RNase, followed by low-speed centrifugation to yield an NE pellet and a supernatant enriched in nuclear contents. In some cases, NEs were resuspended in 10 mM HEPES (pH 7.4)–500 mM NaCl–0.1 mM $MgCl_2$–1 mM dithiothreitol (DTT)–10% sucrose and centrifuged to release most of the contaminating chromatin into a supernatant. To carry out nuclease-salt fractionation of NRK cells, $2 \times 10^7$ cells were collected by trypsinization and washed with PBS. The cells were permeabilized by subjecting the pellet to two freeze-thaw cycles using liquid nitrogen. The cells were then resuspended in 0.5 ml of buffer containing 10 mM HEPES, 10 mM potassium acetate, 2 mM $MgCl_2$, and 1 μg each of leupeptin, pepstatin, and aprotinin per ml. Next, DNase I and RNase A were added to a final concentration of 25 μg/ml, and samples were incubated for 20 min at room temperature (RT). NaCl was then added to a final concentration of 500 mM, and the sample was centrifuged at 20,000 × *g* for 5 min to yield a supernatant and pellet.

To obtain samples of various rat tissues for immunoblot analysis, the tissues (heart, kidney, liver, spleen, and testis) were obtained by dissection, chopped into small pieces in PBS containing 1 mM PMSF and 1 μg each of leupeptin, pepstatin, and aprotinin per ml, homogenized with a Potter-type homogenizer using a motorized Teflon pestle, and boiled in SDS-gel sample buffer. Alternatively, small pieces of tissue were frozen in liquid nitrogen, ground into a powder with a mortar and pestle, and boiled in SDS gel sample buffer (37).

To analyze subcellular fractions and tissue samples by immunoblotting, the samples were electrophoresed on an 8% SDS gel and transferred to a nitrocellulose membrane (Micron Separations, Inc., Westborough, Mass.) (37). The membrane was incubated for 1 h at RT either with 5% nonfat dry milk in PBS or with 3% bovine serum albumin (BSA) in PBS containing 0.1% Triton X-100 and then incubated with affinity-purified antibodies (at 0.5 μg/ml) for 1 h at RT in PBS containing 0.1% Triton X-100 and BSA. After incubation with an alkaline phosphatase-conjugated secondary antibody in PBS-Triton-BSA, the membrane was washed in PBS and developed with a 2:1 mixture of nitroblue tetrazolium and 5-bromo-4-chloro-3-indolyl phosphate (Sigma, St. Louis, Mo.). Alternatively, the membrane was incubated with a horseradish peroxidase-conjugated secondary antibody in PBS-Triton-BSA, and the antibody was detected using the Supersignal West Pico Lumino/Enhancer solution (Pierce Chemical Co., Rockford, Ill.).

**Immunofluorescence microscopy and microinjection.** For indirect immunofluorescent staining, NRK cells were grown on coverslips in Dulbecco modified Eagle medium containing 10% fetal bovine serum, and isolated rat liver nuclei (16) were absorbed to polylysine-coated glass coverslips by incubating them for 30 min on ice. The coverslips first were fixed with 4% formaldehyde in PBS for 6 min at RT and then were permeabilized by incubating them for 6 min on ice with 0.1% Triton X-100 in PBS. For an alternative fixation-permeabilization method, NRK cells were incubated for 30 min at −20°C in methanol, followed by 1 min in ice-cold acetone (10). After fixation and permeabilization, the coverslips were incubated for 30 min at RT in PBS containing 0.1% BSA with either affinity-purified anti-Nup50 (~0.5 μg/ml) or a mixture of anti-Nup50 and the mouse monoclonal antibody RL1 (~1 μg/ml; Affinity BioReagents, Golden, Colo.), which recognizes several glycoproteins of the NPC (37). After incubation with appropriate fluorescently labeled secondary antibodies in PBS containing 0.1% BSA, the coverslips were washed in PBS and mounted with Fluoromount G (Electron Microscopy Sciences, Fort Washington, Pa.). Specimens were examined with a Zeiss Axiophot microscope or a Bio-Rad MRC 1024 laser scanning confocal module attached to a Zeiss Axiovert S100 TV microscope. In the latter case, data were analyzed with LaserSharp version 3.2 software (Bio-Rad, Hercules, Calif.).

For immunofluorescent staining of rat liver cryosections, fresh liver was cut into cubes of ca. 1 to 2 mm, and the pieces were fixed with 4% formaldehyde in PBS for 1 h at RT. Fixed tissue pieces were placed in Tissue-Tek (VWR, San Diego, Calif.) and frozen in liquid nitrogen. Sections (6 to 8 μm) were cut using a Cryocut 1800 (Leica, Heidelberg, Germany) at −18°C and mounted onto

Colorfrost/Plus slides (Fisher, Pittsburg, Pa.). The sections were allowed to dry and then processed for immunofluorescence microscopy as described above.

For the NRK cell microinjection studies, purified GST-NES (2 mg/ml, final concentration) and fluorescein isothiocyanate (FITC)-labeled 150-kDa dextran (2 mg/ml, final concentration) were mixed with anti-Nup50 antibodies (2 mg/ml, final concentration) in microinjection buffer (see above). In some cases the recombinant histidine-tagged Nup50 fragment (residues 173 to 357) was added to the solution to a final concentration of 2 mg/ml. This mixture was introduced into the nucleus of NRK cells at RT by microinjection with a glass needle. The cells were then returned to a 37°C incubator for 30 min. They then were fixed with 4% formaldehyde for 6 min at RT, permeabilized with 0.1% Triton X-100, and labeled for indirect immunofluorescence microscopy to detect the GST-labeled substrate with anti-GST antibodies (Pharmacia Biotech, Piscataway, N.J.). In experiments that monitored nuclear import, the anti-Nup50 and FITC-labeled dextran were injected into the nucleus first, and GST-NLS was subsequently injected into the cytoplasm. After incubation at 37°C for 5 or 30 min, the cells were fixed, and GST-NLS was detected by indirect immunofluorescence microscopy as described above.

**Immunogold electron microscopy.** To localize Nup50 at the electron microscopy level, we carried out pre-embedding immunogold labeling with anti-Nup50 antibody 1 on isolated rat liver NEs or NRK cells. To permeabilize the NRK cell, NRK cell pellets were subjected to a single cycle of freeze-thawing in liquid nitrogen. Suspensions of isolated NE (~200 $A_{260}$ U/ml; see reference 16) or permeabilized NRK cells (~$10^6$ cells/ml) were incubated with affinity-purified anti-Nup50 antibody 1 (5 μg/ml) for 2 h at RT. In some experiments, isolated NEs were incubated with a mixture of anti-Nup50 antibodies (5 μg/ml) and RL11 (10 μg/ml), a mouse monoclonal antibody that recognizes Nup153 (37) for 2 h at RT in PBS containing 0.1% BSA. After being washed in PBS by pelleting and resuspension, samples were incubated with goat anti-rabbit immunoglobulin G conjugated with 5-nm gold particles or a mixture of goat anti-mouse conjugated with 5-nm gold particles and goat anti-rabbit conjugated with 10-nm gold particles (Sigma, St. Louis, Mo.). The samples were incubated for 2 to 3 h at RT, washed, fixed in glutaraldehyde and osmium tetroxide, and embedded in Epon, as described previously (18). Electron micrographs were recorded with a Hitachi 600 electron microscope at 80 kV or a Philips EM-208 at 70 kV.

**Immunoprecipitation and in vitro binding.** To identify proteins bound to Nup50 in NRK cells, $4 \times 10^6$ NRK cells were permeabilized with digitonin (2) and then solubilized in 1 ml of buffer containing 1% NP-40, 50 mM Tris-HCl (pH 8.0), 300 mM NaCl, 5 mM EDTA, 5 mM EGTA, 15 mM $MgCl_2$, 60 mM β-glycerophosphate, 2 mM DTT, and 1 μg each of leupeptin, pepstatin, and aprotinin per ml. After centrifugation for 30 min at 100,000 × *g*, purified anti-Nup50 was added to the solubilized cell supernatant to 5 to 10 μg/ml, and the sample was incubated for 2 h at 4°C. Subsequently, the antibodies were collected by binding to protein A-Sepharose (Pharmacia Biotech), and the immunoprecipitated proteins were analyzed by SDS-PAGE and immunoblotting (see above) with anti-CRM1 (24) or anti-CAS (Transduction Laboratories, Inc., Lexington, Ky.) polyclonal antibodies, or anti-importin-β (Affinity BioReagents) monoclonal antibodies. To analyze in vitro binding of recombinant nuclear transport receptors to the recombinant Nup50 fragment (residues 173 to 357), the Nup50 fragment was coupled to CNBr-activated Sepharose 4B beads (0.5 mg/ml). Purified, His-tagged CRM1, CAS, or importin β were added at 20, 16, or 20 μg/ml, respectively, in the presence or absence of cytochrome *c* coupled with a leucine-rich NES of Rev (100 μg/ml) and Ran preloaded with 25 μg of GMP-PNP (24) per ml and incubated for 80 min at RT. The beads and supernatant were collected and analyzed by SDS-PAGE and immunoblotting as described above, using an anti-His tag antibody (Qiagen, Valencia, Calif.) to detect the transport receptors.

**Mass spectroscopy analysis.** Immunoprecipitation of NRK cells using anti-Nup50 antibody 1 yielded 2 protein bands migrating at about 50 and 70 kDa on an SDS–10% gel. Unstained gel strips having the same mobility as p50 and p70 in Coomassie blue-stained lanes were excised, immersed in a solution of 25 mM ammonium bicarbonate and 50% acetonitrile, and shaken for 10 min. The solution was removed, and the gel strips were rinsed in the same solution. The samples were then completely dried under a stream of nitrogen for 20 min. The gel pieces were rehydrated in the same solution, and 0.5 mg of modified sequence grade trypsin (Promega, Madison, Wis.) dissolved in the same buffer was added to each tube. The samples were incubated overnight with agitation at 30°C. The supernatants were transferred into new Eppendorf tubes for analysis by mass spectrometry. The sample was analyzed on an α-cyano-4-hydroxy-cinnamic acid matrix with a Voyager-DE STR mass spectrometer using the MALDI (matrix-assisted laser desorption ionization) technique and a time-of-flight analyzer (7, 19). Because a reflectron was not used, an error of 0.1% was possible, and mass peaks above 3,000 mass units were not included in the mass alignment.

**Nucleotide sequence accession number.** The GenBank accession number for the corrected sequence of rat Nup50 is U41845.

## RESULTS

**Biochemical characterization of Nup50 and a related antigen.** A cDNA for an NPC-associated protein, termed NPAP60, has been cloned from a rat testis expression library (10). The cDNA sequence predicted a protein consisting of 381 amino acids with a largely hydrophilic character and five FG repeat motifs. We have subsequently detected a frameshift error in the original cDNA sequence at codon 357. The corrected cDNA sequence predicts a protein of 467 amino acids. It is identical to the previously published sequence of amino acids 1 to 356 of NPAP60 (10) but differs in the remaining C-terminal amino acids. Since this protein is tightly associated with the NPC (see below), we designated the protein Nup50, in accordance with the convention for naming nucleoporins. This corrected sequence is highly homologous throughout its length to the sequence of human NPAP60L (41) and mouse Nup50 (36a). The five FG repeat motifs of Nup50 are scattered in the region between residues 76 and 303. Interestingly, the new C-terminal extension assigned to Nup50 after correction of the frameshift error reveals a sequence of ~100 amino acids that is about 30% identical to the RanGTP-binding domains found in RanBP1 and Nup358-RanBP2, as described for the mouse Nup50 (36a).

Nup50 previously was found to be highly expressed in the testis and also was detectable in the rat 1A fibroblast cell line by immunofluorescence staining (10), although the protein was not seen in most other rat cells and tissues by immunoblotting. We now have reinvestigated whether Nup50 is widely expressed in rat cells and tissues using two sets of affinity-purified polyclonal antibodies (Fig. 1). Immunoblot analysis of whole tissue lysates with a polyclonal antibody directed against an internal segment of rat Nup50 (designated antibody 1) (Fig. 1A) detected a major ~50-kDa band corresponding to Nup50 in testis, as originally described, and also revealed a major Nup50 band in liver and spleen. In kidney, an ~70-kDa band (termed p70) was found in addition to Nup50, whereas p70 was the only detectable immunoreactive species in the heart. Antibody 1 also detected Nup50 in whole-cell lysates of three additional rat cultured cell lines besides rat 1A (Fig. 1B). In one of these lines (NRK cells), p70 was seen as well as Nup50, whereas in two of the lines (BRL and HTC), a higher-molecular-weight immunoreactive band also was detected. A different polyclonal antibody raised against recombinant mouse Nup50 (antibody 2) detected only Nup50 in all four cultured cell lines (Fig. 1B). These data indicate that the ~50-kDa band corresponding to Nup50 is present in many different rat cells and tissues. In addition, other immunoreactive species (especially p70) are seen in some cells.

To determine whether p70 is related in sequence to Nup50, we carried out MALDI mass spectrometry (7, 19) on proteolytic digests of the 50- and 70-kDa bands obtained from immunoprecipitates of NRK cells. When the masses of peptides derived from the Nup50 and p70 bands were compared to the predicted sequence of Nup50, we found that numerous peptides obtained from the Nup50 band can be assigned to regions of the predicted Nup50 sequence, as expected (Fig. 2). Furthermore, many peptides derived from the p70 band also can be matched to regions of the Nup50 sequence. From this analysis, we conclude that Nup50 and p70 have regions that are closely related in sequence. However, it is not possible to judge the precise degree of relatedness of these two polypeptides from this analysis, since many peptide fragments were not detectable due to limits in sensitivity. Despite their structural similarity, p70 and Nup50 are the products of distinct genes because p70 is detectable by Western blotting of cultured cell lysates derived from Nup50 null mice (36a).

**Localization of Nup50 in cultured cells and liver nuclei.** We characterized the localization of Nup50 by confocal immunofluorescence microscopy in the cell types we have used for more-detailed analysis in this study (Fig. 3). When formalde-

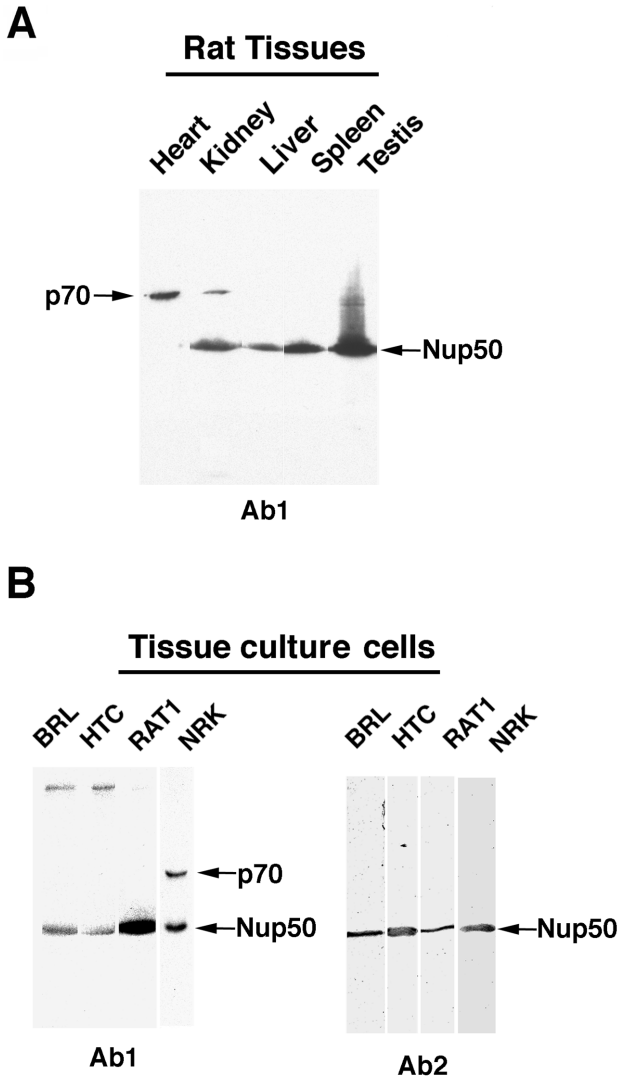


FIG. 1. Immunoblot analysis of Nup50 antigens in various cell lines and tissues from rats. Samples of various rat tissues (A) or cultured cell lines (B), as indicated, were analyzed by immunoblotting with antibody 1 (panel A and the left part part of panel B) and antibody 2 (the right part of panel B). The positions of Nup50 and the major ~70-kDa antigen that is recognized by antibody 1 are indicated.

hyde-fixed cytosections of rat liver were labeled with antibody 1, we obtained moderately strong staining throughout many regions of the nuclear interior, as well as at the NE, as indicated by an overlap with the nuclear rim staining obtained with anti-lamin antibodies (Fig. 3A). However, a number of intranuclear zones, which may include nucleoli, were not strongly labeled. In contrast, when isolated rat liver nuclei were stained with antibody 1, we obtained no significant staining of the nuclear interior and only detected labeling of the NE, a finding similar to the pattern obtained with RL1 (37), a monoclonal antibody that reacts with a group of NPC glycoproteins (Fig. 3B). A similar pattern was obtained with antibody 2 (data not shown). The difference in staining between isolated rat liver nuclei and rat liver cryosections suggests that Nup50 is extracted from internal nuclear regions during the nuclear isolation procedure and preferentially remains attached to the NE.

In NRK cells that were fixed with formaldehyde, both antibody 1 (Fig. 3C, F panels) and antibody 2 (Fig. 3D, F panels) labeled the nucleus quite uniformly, except in regions containing the nucleoli, which showed relatively low levels of staining. The lack of pronounced NE staining (relative to the nuclear interior) in formaldehyde-fixed NRK cells stained with anti-Nup50 antibodies contrasts with the pattern obtained with RL1, which labeled the NE of NRK cells much more strongly than the nuclear interior (Fig. 3C and D, F panels). By contrast, when NRK cells were fixed with methanol-acetone as described previously (10), both antibody 1 (Fig. 3C, M panels) and antibody 2 (Fig. 3D, M panels) yielded prominent NE staining, although a significant level of intranuclear staining was still apparent. Under the same conditions, RL1 labeled predominantly the NE (Fig. 3C and D, M panels). Considering the results obtained with rat liver cryosections and nuclei (above), it is likely that the difference between the labeling of NRK cells obtained with the two fixation conditions reflects the preferential extraction or masking of intranuclear Nup50-related antigens in cells fixed with methanol-acetone compared to formaldehyde. Although anti-Nup50 antibodies did not yield pronounced NE staining of most interphase cells when cells were fixed with formaldehyde, strong NE staining was apparent in late mitotic cells following NE reassembly (Fig. 3C, F panels, pair of telophase cells in upper right). This was similar to the staining pattern seen for late mitotic cells after methanol/acetone fixation (Fig. 3C, M panels, pair of telophase cells in left).

We next examined the intracellular distribution of Nup50 and p70 in rat liver and NRK cells by subcellular fractionation. When rat liver nuclei, which contain only Nup50, were digested with DNase-RNase to release nuclear contents from the NEs, Nup50 appeared mostly in the pellet after centrifugation (Fig. 4A, compare lanes Sup and Pel), similar to other NE markers (data not shown; see also reference 37). Upon subsequent treatment of the NE fraction with 0.5 M NaCl to release the cofractionating chromatin into the supernatant, most of Nup50 appeared in the pellet after centrifugation (Fig. 4B, compare lanes Sup and Pel), a result similar to that for the RL1 antigens

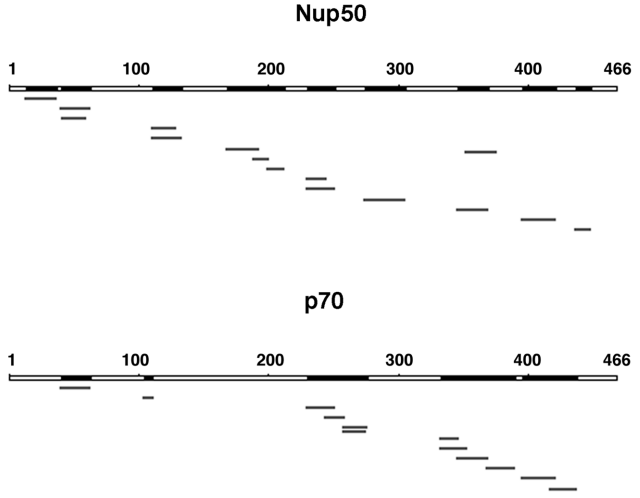


FIG. 2. MALDI mass spectrometry analysis of Nup50 and p70 antigens of NRK cells. Gel-purified Nup50 and p70 bands from anti-Nup50 immunoprecipitates of NRK cells were digested with trypsin, and the products were analyzed by MALDI time-of-flight mass spectrometry. Short bars indicate peptides smaller than 3,000 Da from each band that match (within experimental accuracy) the predicted mass of peptides from the deduced cDNA sequence of rat Nup50. The total regions of the predicted sequence of Nup50 that are represented by peptides obtained in the MALDI analysis are indicated by filled regions of the top bar designating the linear sequence of Nup50.

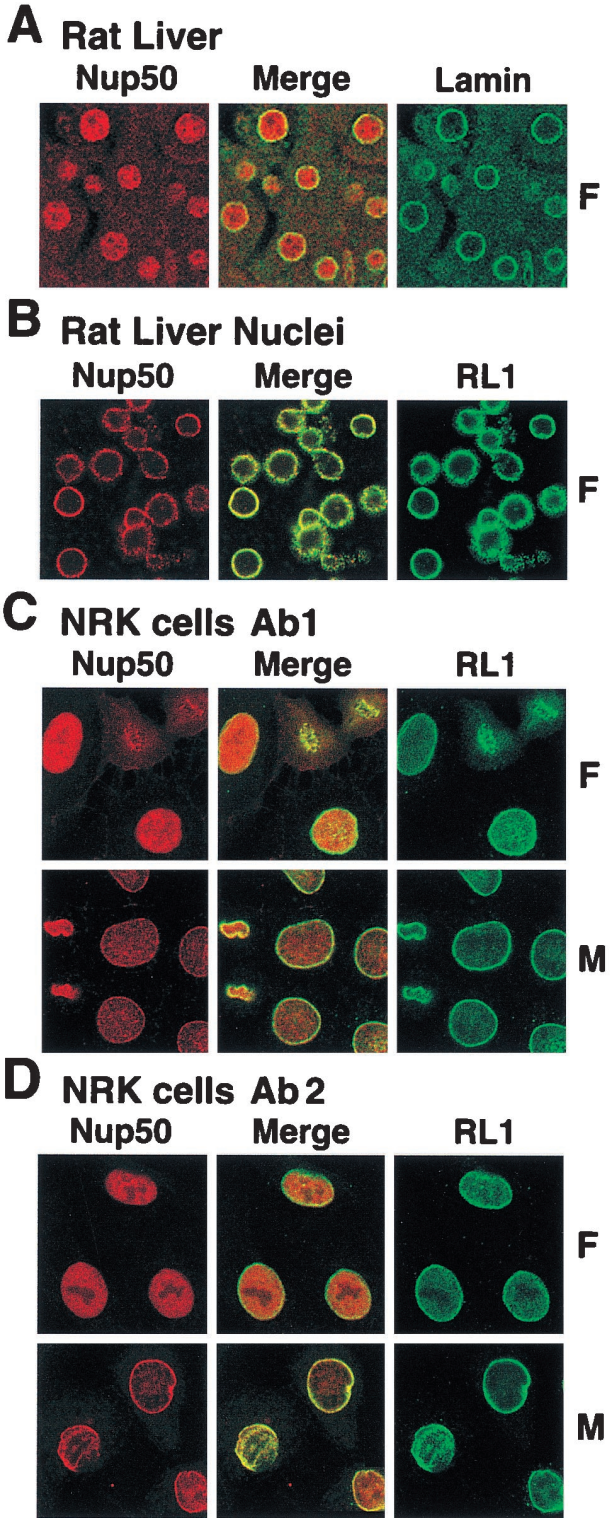


FIG. 3. Immunofluorescent staining of rat liver nuclei and NRK cells with anti-Nup50 antibodies. Rat liver cryosections (A), isolated rat liver nuclei (B), or NRK cells (C and D) were fixed with either formaldehyde (F panels) or methanol-acetone (M panels) and labeled with antibody 1 (A to C) or antibody 2 (D) against Nup50 for visualization by indirect immunofluorescence microscopy.

(Fig. 4B, compare lanes Sup and Pel). These results indicate that Nup50 is tightly associated with the NE of rat liver, a result consistent with the preferential retention of Nup50 at the NE during nuclear isolation (see Fig. 3). We also carried out an analogous fractionation scheme on NRK cells, which contain both Nup50 and p70. Lysed cells were digested with DNase-RNase, the digestion mixtures were treated with 0.5 M NaCl, and the mixtures were centrifuged to yield a pellet fraction containing NEs and other insoluble intranuclear and cytoplasmic material and a supernatant containing extracted proteins. In this case, a majority of p70 and about half of the Nup50 appeared in the pellet compared to the supernatant (Fig. 4C, compare lanes Sup and Pel). The majority of the NPC marker protein Nup153 also appeared in the pellet fraction (Fig. 4C, compare lanes Sup and Pel). These data support the possibility that a major fraction of both Nup50 and p70 interact strongly with the NE of cultured NRK cells, as with rat liver cells. The increased fraction of Nup50 that is extractable with a high salt concentration from NRK cells compared to rat liver nuclei may reflect the large intranuclear pool of this protein in NRK cells that is not evident in liver nuclei by immunofluorescence microscopy. Nup50 solubilized from rat liver NE did not bind to the lectin wheat germ agglutinin (WGA) and appeared exclusively in the unbound fraction (Fig. 4D, compare lanes unbd and bd). This result is distinct from all of the other well-characterized FG repeat nucleoporins of rat liver, which bind to WGA due to modification with *O*-linked *N*-acetylglucosamine (11, 21).

To localize the NE-associated Nup50-p70 antigens at a higher resolution, we first examined the accessibility of these antigens to antibodies in digitonin-permeabilized NRK cells, which retain an intact NE (2). In this situation, only proteins on the cytoplasmic surface of the NPC are available for antibody binding, since antibody molecules are too large to diffuse through the NPC. Whereas strong labeling of the NE of digitonin-treated cells was obtained with RL1, which recognizes cytoplasmic and nucleoplasmic NPC antigens (37), no staining was obtained with antibody 1 against Nup50-p70 (data not shown). In contrast, when cells were treated with Triton X-100 to permeabilize the NE prior to incubation with the antibodies, strong labeling of the NE was obtained with antibody 1. These data suggest that Nup50 and p70 are restricted to the nucleoplasmic side of the NPC.

To more decisively determine the localization of Nup50 and p70, we used immunogold electron microscopy to label Nup50 in isolated rat liver NE and in NRK cells that were permeabilized by freeze-thawing (Fig. 5). In rat liver NE, anti-Nup50 antibodies labeled the nucleoplasmic surface of the NPC almost exclusively (Fig. 5A, arrowheads in left panel). In tangential views (Fig. 5A, right panels, arrowheads), rings of gold labeling were sometimes seen, a result reminiscent of antigens that are localized in the terminal ring structure of the nucleoplasmic basket of the NPC (30, 34). The labeling pattern obtained with anti-Nup50 closely resembled that obtained with an anti-Nup153 monoclonal antibody (RL11) in double immunogold labeling (Fig. 5B). Quantification of the labeling obtained with the two antibodies (Fig. 5D) showed that most gold particles for both anti-Nup50 and anti-Nup153 occurred at between 15 and 80 nm of the midplane of the NPC, with a strong peak at 35 to 45 nm. These data indicate that Nup50 is located at or near the nucleoplasmic fibrils of the NPC in rat liver, where Nup153 has been previously localized.

In NRK cells, anti-Nup50 antibodies yielded gold labeling at both the nucleoplasmic side of the NPC and in the nuclear interior (Fig. 5C; arrowheads indicate gold in the nuclear interior). Quantification of the NPC labeling in these cells (Fig.

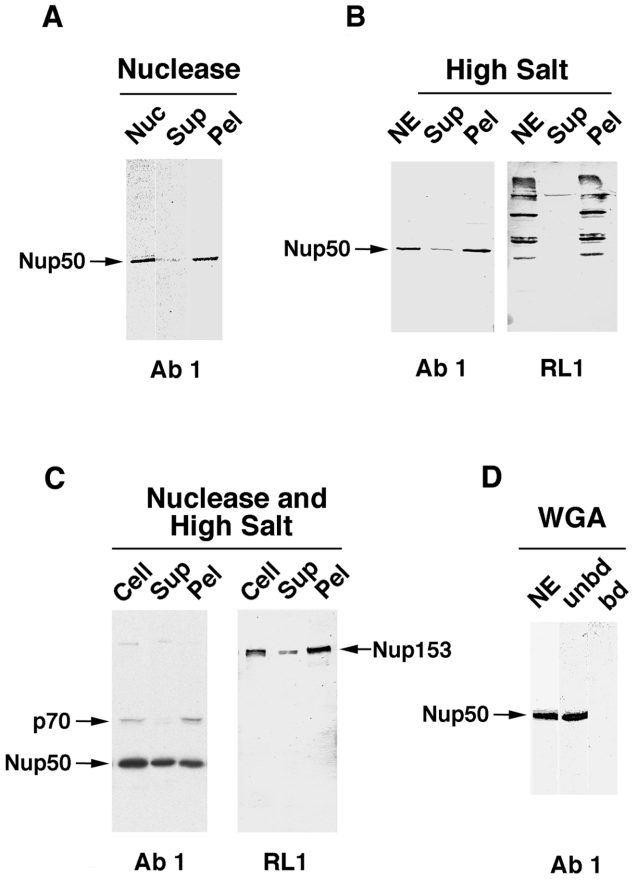


FIG. 4. Distribution of Nup50 by subcellular fractionation. (A) Isolated rat liver nuclei (Nuc) were digested with DNase-RNase to release intranuclear contents from the NE and were centrifuged at low speed to yield a supernatant (Sup) and pellet (Pel). (B) Isolated rat liver NE, derived by nuclease-salt extraction of nuclei, were suspended in a solution containing 0.5 M NaCl and were centrifuged to yield a supernatant and a pellet. (C) NRK cells (Cell) were permeabilized, digested with DNase-RNase, suspended in buffer containing 0.5 M NaCl, and centrifuged to yield a supernatant and pellet. (D) Rat liver NEs were solubilized in nonionic detergent buffer and were passed over a WGA affinity column, yielding bound and unbound fractions. Samples of the various subcellular fractions were electrophoresed on SDS gels and analyzed by immunoblotting with antibody 1 or the monoclonal antibody RL1 as indicated.

5E) showed that the gold occurred at between 20 and 100 nm of the midplane of the NPC, with a strong peak at 40 to 50 nm. The slightly greater average distance of the labeling from the NPC midplane in this case is consistent with the possibility that the NPC fibrils are less collapsed in intact nuclei compared to isolated NE. Thus, immunogold electron microscopy of NRK cells confirms the results of immunofluorescence microscopy, indicating that Nup50 is localized to both the nucleoplasmic side of the NPC and in the nuclear interior. Moreover, in NRK cells, as well as in rat liver, Nup50 clearly is concentrated in the nucleoplasmic fibrils of the NPC. Considered together, our immunolocalization data indicate that Nup50 is a bona fide nucleoporin with a distinctive localization in the three-dimensional structure of the NPC (see Discussion).

**Role of Nup50 in nuclear protein export.** We microinjected affinity-purified anti-Nup50 antibodies into the nuclei of cultured NRK cells to investigate a possible involvement of Nup50 in nuclear protein export and import. We examined the effects of antibody 1, which recognizes both Nup50 and p70 in NRK cells, as well as antibody 2, which is specific for Nup50 in this cell type (see Fig. 1). In the nuclear export studies (Fig. 6), anti-Nup50 antibodies were injected into the cell nucleus together with a GST-NES substrate molecule (containing a leucine-rich NES) and a large fluorescent dextran to mark the injected nuclei. After 30 min, cells were fixed and then examined by immunofluorescent microscopy to evaluate the nuclear-cytoplasmic distribution of the GST-NES substrate. In control cells injected with only buffer instead of anti-Nup50 antibodies (Fig. 6A), the GST-NES became concentrated in the cytoplasm, a result indicative of efficient nuclear export, whereas the large dextran remained confined to the nuclear interior. In contrast, in cells injected with either antibody 1 or antibody 2 (Fig. 6B and C), most of the substrate remained confined to the nuclear interior, a finding indicative of strong inhibition of nuclear export. However, if cells were injected with a mixture of antibody 1 and an excess of the corresponding antigen used for immunization, efficient export of the substrate now occurred (Fig. 6D), confirming that the inhibition of export was antigen specific. Thus, both antibodies strongly inhibited export of a protein containing a leucine-rich NES in NRK cells.

We next examined the effects of the antibodies on nuclear import of a GST-NLS substrate molecule (containing a classical, basic-amino-acid-rich NLS). In this case, the anti-Nup50 antibodies plus fluorescent dextran first were injected into the nucleus of NRK cells. Subsequently, the GST-NLS cargo was injected into the cytoplasm, the cells were fixed at various times, and the localization of the substrate protein was examined. With cells that had not been preinjected (Fig. 7A), the NLS-containing protein became substantially concentrated in the nucleus by 5 min, although some cargo (variable in relative amounts from cell to cell) was still present in the cytoplasm of most cells. Approximately the same level of nuclear import was obtained after 5 min in cells that were injected with anti-Nup50 antibody 1 instead of buffer (Fig. 7B). After 30 min, essentially all of the detectable NLS cargo protein was imported into the nucleus of cells either not preinjected (Fig. 7A) or preinjected with anti-Nup50 antibody 1 (Fig. 7B). Similar to the results shown for antibody 1, no detectable inhibition of nuclear import of GST-NLS was observed in cells injected with antibody 2 (data not shown). In summary, whereas anti-Nup50 antibodies strongly inhibit nuclear export of a protein with a leucine-rich NES in NRK cells, the antibodies have no effect on nuclear import of a protein with a classical NLS.

The inhibition of nuclear export by anti-Nup50 antibodies suggests that Nup50 may be a binding site for the nuclear export complex containing CRM1 (the receptor that binds leucine-rich NESs) during its passage through the NPC. This finding is consistent with the finding that other FG nucleoporins directly bind a variety of nuclear import and export receptors (reviewed in references 1 and 17). To more directly evaluate this possibility, we first examined whether CRM1 and other nuclear import and export receptors are associated with Nup50 when the latter is immunoprecipitated from nonionic detergent-high-salt extracts of NRK cells (Fig. 8A). Indeed, we found that a significant amount of CRM1 coprecipitated with Nup50, whereas no CAS (the nuclear export receptor for importin $\alpha$) or lamin B (a control NE protein) appeared in the immunoprecipitate. (Note that more cell equivalents of bound than unbound samples are presented in this experiment; see Fig. 8 legend). We also found that a substantial amount of importin $\beta$ appeared in the anti-Nup50 immunoprecipitate. This may reflect either a direct or an indirect interaction between these two proteins. However, since we observed that a significant amount of Nup153 coimmunoprecipitates with Nup50 in cell extracts (data not shown; see also reference 36a)

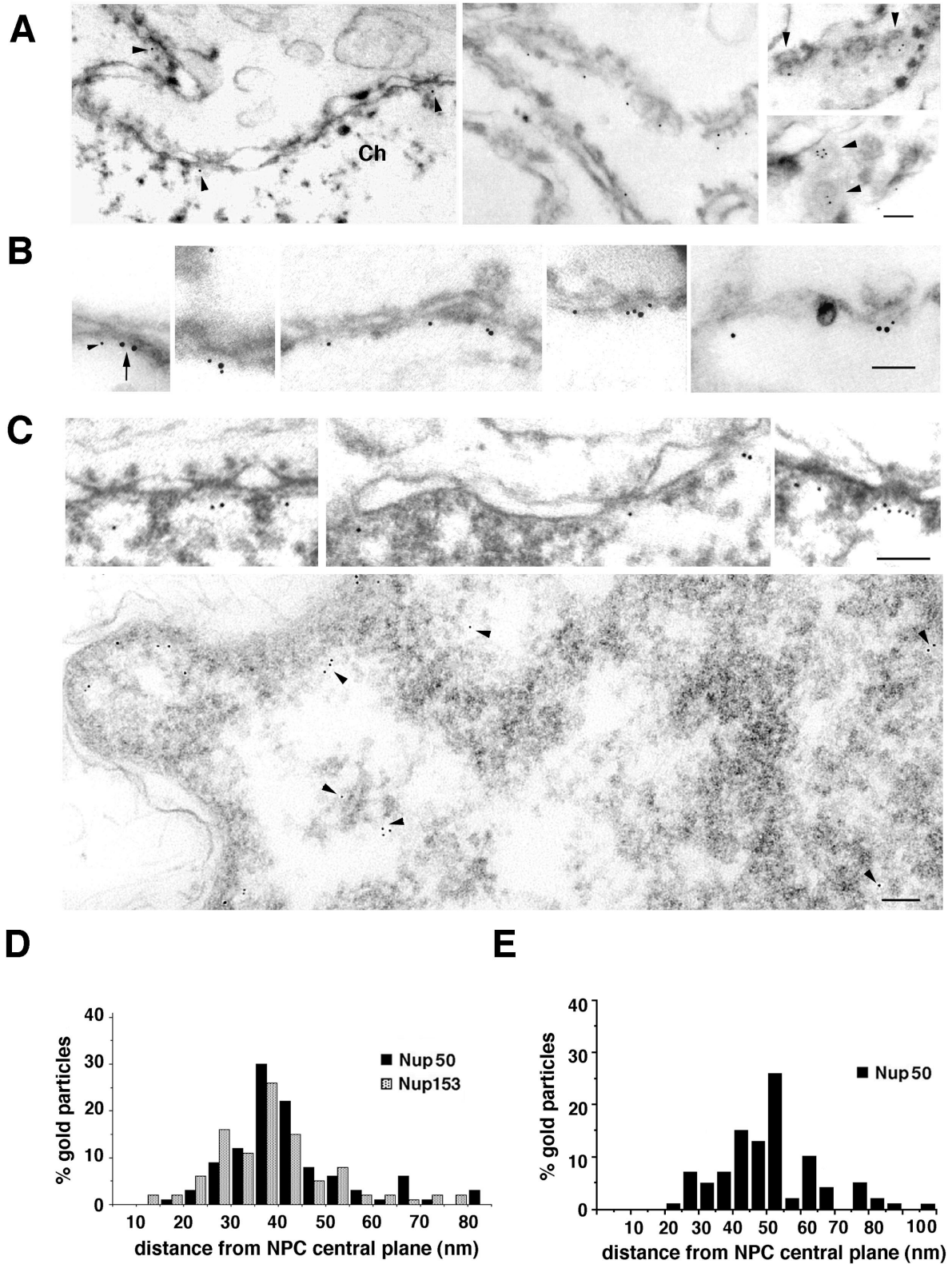


FIG. 5. Immunoelectron microscopic localization of Nup50 in NEs and NRK cells. (A) Isolated rat liver NEs were labeled by indirect immunogold techniques with anti-Nup50 antibodies (antibody 1). Shown are cross-sectional (left two panels) and tangential (right panels) views of the NE depicting the labeling pattern that was obtained. Undigested chromatin associated with the inner nuclear membrane (Ch) allows distinction between the cytoplasmic and nucleoplasmic sides of the NPC. Arrowheads denote NPCs that are labeled with anti-Nup50 antibodies. (B) Isolated rat liver NEs were processed by indirect immunogold labeling to simultaneously localize Nup50 (antibody 1, 10-nm gold, arrow in left panel) and Nup153 (RL11, 5-nm gold, arrowhead in left panel). (C) NRK cells were permeabilized by freeze-thawing, and Nup50 was localized by indirect immunogold labeling. The top row of panels depicts cross-sectional views of the NE, which reveal gold labeling exclusively on the nucleoplasmic side of the NPC. The bottom panel presents a cross-section through the nucleus, showing that gold labeling is present in more internal nuclear regions (arrowheads), as well as at the nucleoplasmic surface of the NPC. Bars, 100 nm. (D) Quantification of the localization of Nup50 and Nup153 in isolated rat liver NEs with respect to the NPC midplane. One hundred eighteen gold particles were counted for Nup50, and 110 were counted for Nup153. (E) Quantification of the localization of Nup50 at the NE of NRK cells with respect to the NPC midplane. Eighty-four gold particles were counted.

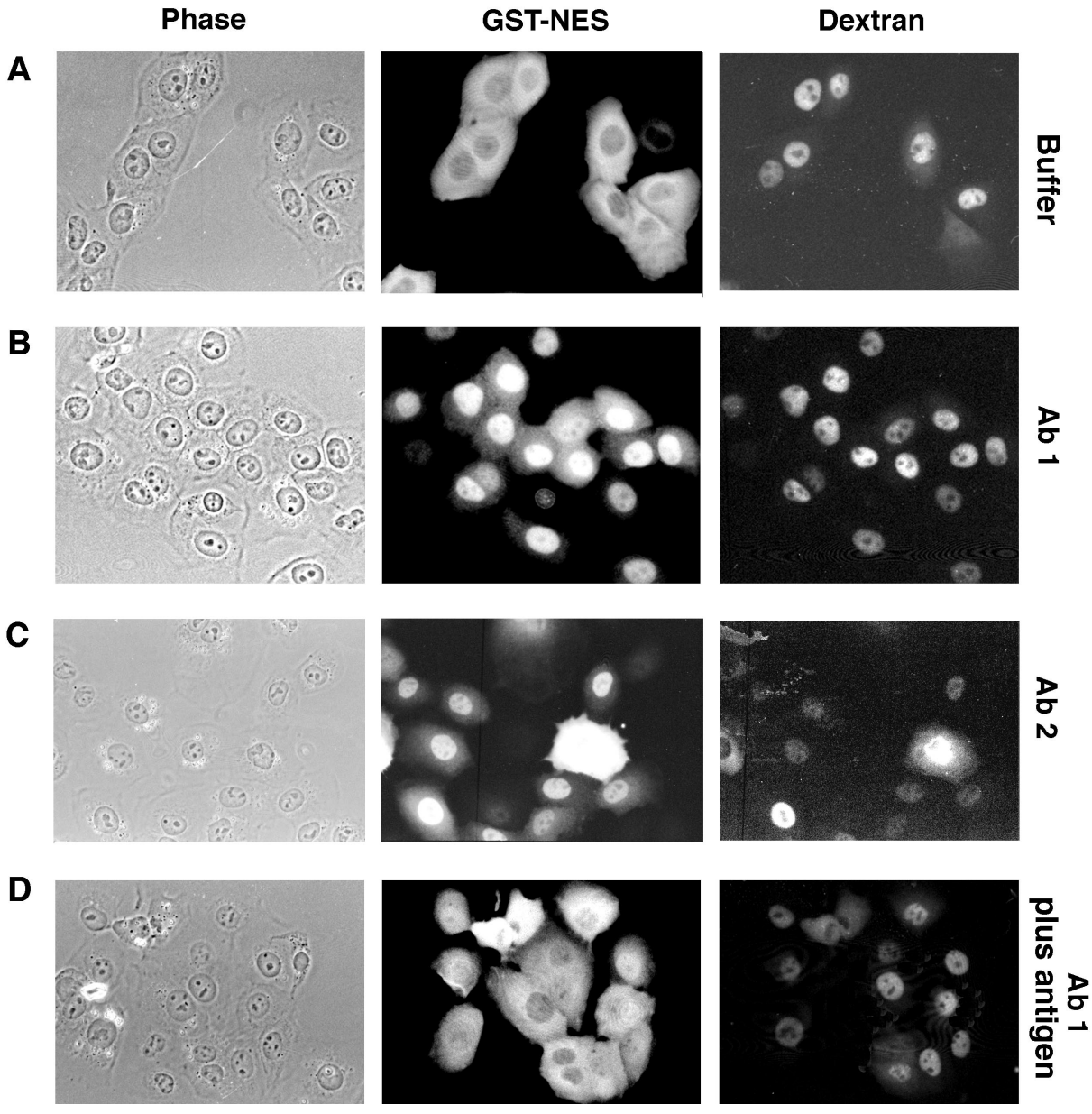


FIG. 6. Analysis of nuclear protein export in NRK cells injected with anti-Nup50 antibodies. The nuclei of cells were injected with a marker 100-kDa fluorescent dextran, together with GST-NES mixed with buffer (A) or with GST-NES mixed with antibody 1 (B), antibody 2 (C), or antibody 1 plus immunizing antigen (D), as shown. After 30 min at 37°C, cells were fixed, and the localization of GST-NES was determined by indirect immunofluorescence microscopy. Injected nuclei are denoted by the fluorescent dextran.

and since Nup153 is a major binding partner of importin β that coprecipitates with the latter in cell extracts (36), we believe that at least part of the importin β in the anti-Nup50 immunoprecipitate is due to its association with coprecipitating Nup153.

To determine whether the association of CRM1 with Nup50 observed in cell immunoprecipitates is direct or indirect, we examined the binding of a variety of recombinant import and export receptors, including CRM1, to a recombinant fragment of Nup50 (comprising residues 173 to 357) that was immobilized on a Sepharose matrix (Fig. 8B). The receptor binding was examined in the absence or presence of RanGTP and/or a cytochrome *c*-NES protein conjugate (cc-NES), which cooperatively bind to CRM1. We observed a substantial level of CRM1 binding to the Nup50 fragment under all conditions, with a slight enhancement of binding when both RanGTP and cc-NES were present. However, there was no substantial binding to the nuclear transport receptors CAS and importin β to the Nup50 fragment under the same conditions (Fig. 8B). Moreover, the recombinant CRM1 did not bind significantly to immobilized BSA. Taken together, these data indicate that CRM1 specifically and directly binds to Nup50 and that the binding occurs in the presence of an excess of RanGTP and cc-NES, when the CRM1 would be assembled into an export complex with the latter. While it remains possible that some other nuclear transport receptors can bind to full-length

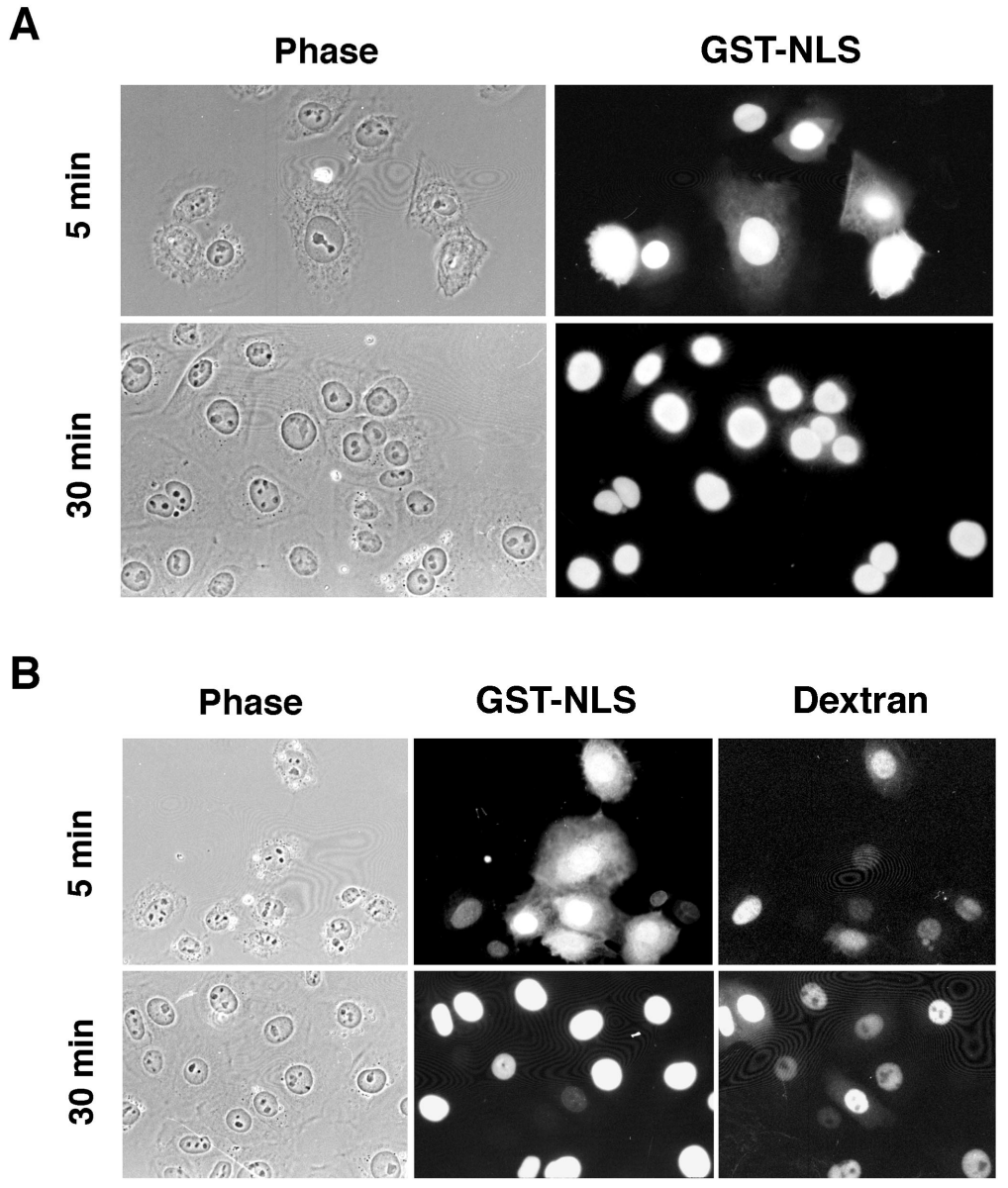


FIG. 7. Analysis of nuclear protein import in NRK cells injected with anti-Nup50 antibodies. (A) Cells were injected in the cytoplasm with GST-NLS. After either 5 or 30 min at 37°C, cells were fixed and the GST-NLS was localized by indirect immunofluorescence microscopy. (B) Cells were injected into the nucleus with a mixture of a marker (100-kDa fluorescent dextran) and antibody 1. They were then injected into the cytoplasm with GST-NLS. After either 5 or 30 min at 37°C, cells were fixed and the GST-NLS was localized by indirect immunofluorescence microscopy. Injected nuclei are denoted by the fluorescent dextran.

Nup50, these data nevertheless indicate that CRM1 binds selectively to the fragment of Nup50 that we have examined.

The observation that the binding of Nup50 to CRM1 is not diminished by an excess of a NES-containing export cargo (Fig. 8B) argues that Nup50 is not itself a cargo for CRM1, whose binding to the NPC is mediated by this cargo receptor. To further test this possibility, we examined whether Nup50 remains stably associated with the NPC upon incubation of cells with leptomycin B, a drug that blocks the binding of cargo molecules to CRM1 (13, 15, 29) but not the export of CRM1 from the nucleus in vivo (13) or in vitro (unpublished observations). As shown in Fig. 8C, there was no decrease in the level of Nup50 associated with the NE of cultured cells after 4 h of incubation in leptomycin B, a finding similar to that for the NPC proteins recognized by the RL1 monoclonal antibody. This further supports the possibility that Nup50 is a nucleoporin binding site for CRM1 during nuclear transport.

## DISCUSSION

In this study we have shown that Nup50, an NPC-associated protein that was previously described in rat cultured cells and spermatocytes (10), is widely distributed among different rat cell types. Similar findings have been made with mouse Nup50, which was recently detected in a two-hybrid screen with the cdk inhibitor p27(kip1) (36a). We observed that certain rat cells and tissues contain at least one additional polypeptide related to Nup50, notably p70, based on immunoblotting with affinity-purified polyclonal anti-Nup50 antibodies and MALDI mass spectrometry. It is clear that Nup50 and p70 are the products

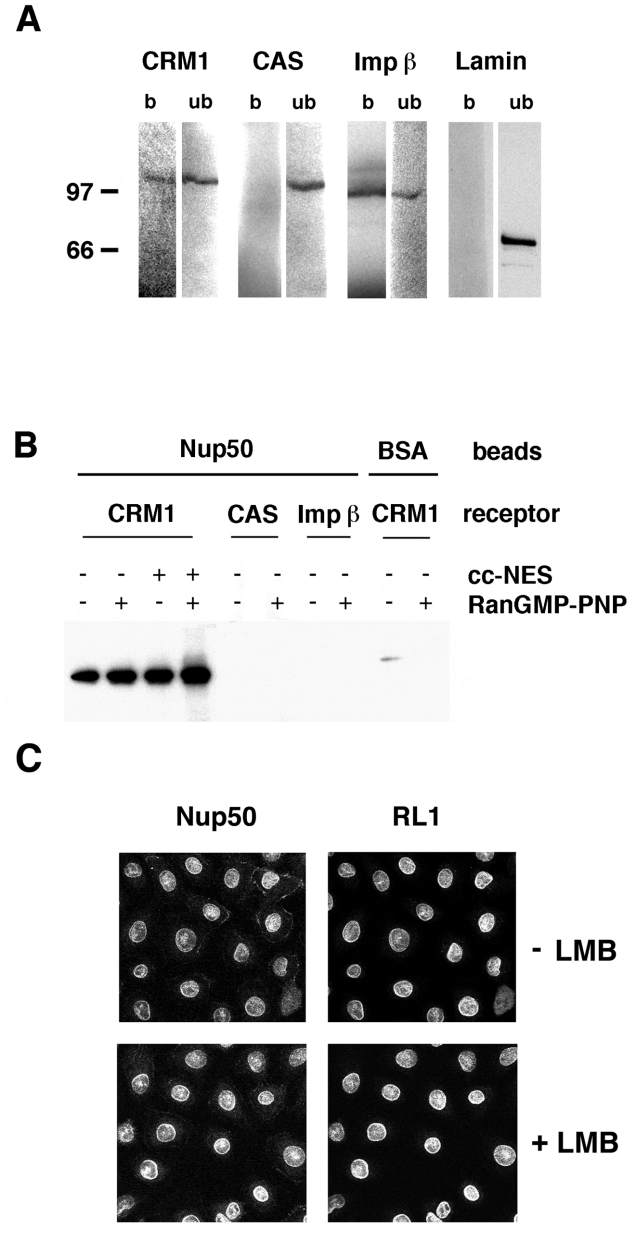


FIG. 8. Interaction of nuclear transport receptors with Nup50. (A) NRK cells were solubilized in NP-40 buffer, and extracts were immunoprecipitated with anti-Nup50 antibodies (antibody 1). Material bound to the antibody beads (b) and the unbound material (ub) were electrophoresed on an SDS gel and analyzed by immunoblotting with anti-CRM1, anti-CAS, anti-importin β, or anti-lamin antibodies. Note that the sample loaded in the bound lanes represents sevenfold more cell equivalents than the material in the unbound lanes. (B) Sepharose beads coupled with a Nup50 fragment (Nup50) or with BSA were incubated with recombinant CRM1, CAS, or importin β in the absence or presence of RanGMP-PNP or cytochrome *c* coupled with NES peptides (cc-NES) as indicated. Samples were analyzed by immunoblotting with antibodies recognizing the $His_6$ tag of the recombinant receptors. An equivalent amount of the bound material was loaded in all cases. Moreover, the input material contained nearly equal quantities of all transport receptors, as determined by protein analysis. (C) NRK cells were incubated at 37°C for 4 h in growth medium containing 100 nM leptomycin B (+LMB) or lacking leptomycin B (−LMB). They were then fixed with methanol-acetone (see Materials and Methods) and examined by confocal microscopy after double immunofluorescence staining with anti-Nup50 (antibody 1) or RL1, as indicated.

of distinct genes, because p70 is detectable by Western blotting of cultured cell lysates derived from Nup50 null mice (36a). The protein family containing these two products may include additional members related by gene duplication or alternative splicing. A cDNA encoding a protein that is related (but not identical) in part of its sequence to Nup50 has been detected in the mouse testis (36a), and multiple human chromosomes have been found to contain sequences that react with human Nup50 probes (41). Moreover, multiple poly(A)$^+$ RNAs homologous to human Nup50-NPAP60L have been detected on Northern blots of various tissues. This group of RNAs arises in part from the utilization of alternative polyadenylation sites at the 3′ end of the gene (41) and also could reflect alternative splicing.

Immunogold electron microscopy of isolated rat liver NEs and NRK cells shows that Nup50 is located at the nucleoplasmic periphery of the NPC, in a region that is similar to the localization region previously described for Nup153 (30). The close colocalization of Nup50 and Nup153 is consistent with the finding that Nup153 is coimmunoprecipitated with Nup50 in detergent extracts of cultured cells (36a; data not shown) and that Nup153 is detected in a two-hybrid screen with mouse Nup50 (36a). The findings that Nup50 is localized to a discrete region of the NPC, that it is tightly bound to the NE, and that its association with the NE in cultured cells is not diminished by incubation with leptomycin B (which blocks cargo binding to CRM1) all argue that Nup50 is a bona fide nucleoporin.

In cultured NRK cells, as well as in rat liver, we detected a relatively high concentration of Nup50 in internal nuclear regions, as well as at the NPC, a finding similar to the localization of mouse Nup50 in mouse embryo fibroblasts (36a). The partial localization of Nup50 to internal nuclear regions in cultured cells is not unusual, since a number of other nucleoporins also have been shown to be localized both to the nuclear interior and at the NE (e.g., references 6 and 12). It is possible that the nucleoplasmic pool of Nup50 dynamically exchanges with the NPC-associated pool, which is perhaps related to a role in nuclear transport. Alternatively, the Nup50 in internal nuclear regions might represent a stockpile or unassembled pool of Nup50 found in rapidly growing cells. The biochemical fractionation of cells is consistent with the notion that p70, like Nup50, is a nucleoporin, although proof of this possibility will require immunolocalization with monospecific antibodies against p70.

We examined the possible role of Nup50 in nuclear transport by microinjecting affinity-purified anti-Nup50 antibodies into the nucleus of NRK cells and subsequently analyzing the nuclear import and export of microinjected substrates. Whereas neither of our anti-Nup50 antibodies had a detectable effect on the rate of nuclear import of a protein substrate containing a classical NLS (that binds to the importin α/β-heterodimer), both antibodies strongly inhibited the export of a substrate with a leucine-rich NES (that interacts with CRM1). The specificity of this inhibition argues for a direct role of Nup50 in CRM1-mediated nuclear export. In further support of this possibility, we found that a recombinant fragment of Nup50 containing several of the FG repeat motifs selectively bound to CRM1 but not to importin β or the export receptor CAS. This binding occurred in the presence of a leucine-rich NES cargo and RanGTP, which form a trimolecular complex with CRM1 that is thought to be involved in nuclear export (13). These findings, together with the inhibition of nuclear export in cultured cells obtained by injection of anti-Nup50 antibodies, argue that Nup50 is a binding site at the NPC for the CRM1 cargo-receptor complex during the process of nuclear export. We found that the in vitro binding of CRM1 to the Nup50 fragment is not inhibited by an excess of antibody 1 (unpub-

lished observations). This suggests that at least this antibody inhibits nuclear export by preventing the transfer of the CRM1-containing export complex to or from Nup50, rather than by inhibiting this binding reaction per se. It has been found that a homozygous mouse null mutation for Nup50 does not cause lethality until late embryogenesis, although Nup50 is expressed ubiquitously during embryogenesis (36a). This suggests that other nucleoporins, such as Nup50 related proteins (see above), can carry out the functions mediated by Nup50 in many embryonic cells or that the Nup50-related step in transport is not essential in many embryonic cell types (see below).

It is conceivable that Nup50 has a role in other nuclear export pathways besides that mediated by CRM1. Moreover, although no inhibition of nuclear import was obtained by injection of anti-Nup50 antibodies and no direct binding of importin β was observed for the fragment of Nup50 that we analyzed, it is possible that Nup50 has a role in nuclear import that remains undetected with these approaches. In this regard, two-hybrid screening with mouse Nup50 revealed interactions with multiple nuclear transport receptors and adaptors, including importin α, importin β, and transportin (36a), although it is not yet known which of these are due to direct binding.

Recent studies have identified a number of vertebrate nucleoporins that can bind nuclear export receptors in vitro (4, 14, 24, 28), and cell transfection and antibody injection studies have implicated some of these in RNA export (5, 32, 42). Among the nucleoporins implicated in nuclear export, Nup214-CAN, p62 complex subunits, and Nup153 have been found to bind to the export receptor CRM1 in a manner stimulated by RanGTP (4, 24, 28), which is consistent with a possibility that these are binding sites for the nuclear export complex during its movement through the NPC. Moreover, Nup214-CAN and the p62 complex are found associated with CRM1 when disassembly of export receptors at the cytoplasmic side of the NPC is inhibited by the use of a Ran mutant locked in the GTP-bound state (24). According to the model that movement of nuclear transport complexes through the NPC occurs by processive transfer between different nucleoporins, the localization of Nup50 at the nucleoplasmic periphery of the NPC suggests that this protein is involved in a more proximal step of export than those involving the p62 complex and Nup214-CAN, which are found in the center and at the cytoplasmic periphery of the NPC, respectively. Presumably, Nup50 acts near the step mediated by Nup153, which also is at the nucleoplasmic periphery of the NPC and apparently is in a macromolecular complex with Nup50 (see above). It will be interesting to determine whether the movement of the CRM1 export complex involves direct transfer from Nup153 (or vice versa). The work we describe in the present study provides a framework for analyzing this question and other issues related to the specific role of Nup50 in nuclear transport.

## ACKNOWLEDGMENTS

This work was supported by a grant from Novartis Pharmaceuticals to L.G., NIH postdoctoral fellowship F32 GM19085 to E.C.S., and NIH grant GM36745 to N.A. B.E.C. is a W. M. Keck Distinguished Young Scholar in Medical Research and is a scholar of the James S. McDonnell Foundation.

We gratefully acknowledge the gifts of cDNA clones from Susan Taylor, Iain Mattaj, and Dirk Görlich.

## REFERENCES

1. **Adam, S. A.** 1999. Transport pathways of macromolecules between the nucleus and the cytoplasm. Curr. Opin. Cell. Biol. **11:**402–406.
2. **Adam, S. A., R. S. Marr, and L. Gerace.** 1990. Nuclear protein import in permeabilized mammalian cells requires soluble cytoplasmic factors. J. Cell Biol. **111:**807–816.
3. **Arts, G. J., M. Fornerod, and I. W. Mattaj.** 1998. Identification of a nuclear export receptor for tRNA. Curr. Biol. **8:**305–314.
4. **Askjaer, P., A. Bachi, M. Wilm, F. R. Bischoff, D. L. Weeks, V. Ogniewski, M. Ohno, C. Niehrs, J. Kjems, I. W. Mattaj, and M. Fornerod.** 1999. RanGTP-regulated interactions of CRM1 with nucleoporins and a shuttling DEAD-box helicase. Mol. Cell. Biol. **19:**6276–6285.
5. **Bastos, R., A. Lin, M. Enarson, and B. Burke.** 1996. Targeting and function in mRNA export of nuclear pore complex protein Nup153. J. Cell Biol. **134:**1141–1156.
6. **Cordes, V. C., S. Reidenbach, H. R. Rackwitz, and W. W. Franke.** 1997. Identification of protein p270/Tpr as a constitutive component of the nuclear pore complex-attached intranuclear filaments. J. Cell Biol. **136:**515–529.
7. **Cotter, R. J.** 1992. Time-of-flight mass spectrometry for the structural analysis of biological molecules. Anal. Chem. **64:**1027A–1039A.
8. **Delphin, C., T. Guan, F. Melchior, and L. Gerace.** 1997. RanGTP targets p97 to RanBP2, a filamentous protein localized at the cytoplasmic periphery of the nuclear pore complex. Mol. Biol. Cell **8:**2379–2390.
9. **Doye, V., and E. Hurt.** 1997. From nucleoporins to nuclear pore complexes. Curr. Opin. Cell Biol. **9:**401–411.
10. **Fan, F., C.-P. Liu, O. Korobova, C. Heyting, H. H. Offenberg, G. Trump, and N. Arnheim.** 1997. cDNA cloning and characterization of Npap60: a novel rat nuclear pore-associated protein with an unusual subcellular localization during male germ cell differentiation. Genomics **40:**444–453.
11. **Finlay, D. R., D. D. Newmeyer, T. M. Price, and D. J. Forbes.** 1987. Inhibition of in vitro nuclear transport by a lectin that binds to nuclear pores. J. Cell Biol. **104:**189–200.
12. **Fontoura, B. M., G. Blodel, and M. J. Matunis.** 1999. A conserved biogenesis pathway for nucleoporins: proteolytic processing of a 186-kilodalton precursor generates Nup98 and the novel nucleoporin, Nup96. J. Cell Biol. **144:**1097–1112.
13. **Fornerod, M., M. Ohno, M. Yoshida, and I. W. Mattaj.** 1997. CRM1 is an export receptor for leucine-rich nuclear export signals. Cell **90:**1051–1060.
14. **Fornerod, M., J. van Deursen, S. van Baal, A. Reynolds, D. David, K. G. Murti, J. Fransen, and G. Grosveld.** 1997. The human homologue of yeast CRM1 is in a dynamic subcomplex with CAN/Nup214 and a novel nuclear pore component Nup88. EMBO J. **16:**807–816.
15. **Fukuda, M., S. Assano, T. Nakamura, M. Adachi, M. Yoshida, M. Yanagida, and E. Nishida.** 1997. CRM1 is responsible for intracellular transport mediated by the nuclear export signal. Nature **390:**308–311.
16. **Gerace, L., C. Comeau, and M. Benson.** 1984. Organization and modulation of nuclear lamina structure. J. Cell Sci. Suppl. **1:**137–160.
17. **Gorlich, D., and U. Kutay.** 1999. Transport between the cell nucleus and the cytoplasm. Annu. Rev. Cell Dev. Biol. **15:**607–660.
18. **Guan, T., S. Muller, G. Klier, N. Pante, J. M. Blevitt, M. Haner, B. Paschal, U. Aebi, and L. Gerace.** 1995. Structural analysis of the p62 complex, an assembly of *O*-linked glycoproteins that localizes near the central gated channel of the nuclear pore complex. Mol. Biol. Cell **6:**1591–1603.
19. **Hillenkamp, F., M. Karas, R. C. Beavis, and B. T. Chait.** 1991. Matrix-assisted laser desorption/ionization mass spectrometry of biopolymers. Anal. Chem. **63:**1193A–1203A.
20. **Hinshaw, J. E., B. O. Carragher, and R. A. Milligan.** 1992. Architecture and design of the nuclear pore complex. Cell **69:**1133–1141.
21. **Holt, G. D., C. M. Snow, A. Senior, R. S. Haltiwanger, L. Gerace, and G. W. Hart.** 1987. Nuclear pore complex glycoproteins contain cytoplasmically disposed O-linked *N*-acetylglucosamine. J. Cell Biol. **104:**1157–1164.
22. **Hu, T., T. Guan, and L. Gerace.** 1996. Molecular and functional characterization of the p62 complex, an assembly of nuclear pore complex glycoproteins. J. Cell Biol. **134:**589–601.
23. **Jarnik, M., and U. Aebi.** 1991. Toward a more complete 3-D structure of the nuclear pore complex. J. Struct. Biol. **107:**291–308.
24. **Kehlenbach, R. H., A. Dickmanns, A. Kehlenbach, T. Guan, and L. Gerace.** 1999. A role for RanBP1 in the release of CRM1 from the nuclear pore complex in a terminal step of nuclear export. J. Cell Biol. **145:**645–657.
25. **Kutay, U., G. Lipowsky, E. Izaurralde, F. R. Bischoff, P. Schwarzmaier, E. Hartmann, and D. Gorlich.** 1998. Identification of a tRNA-specific nuclear export receptor. Mol. Cell **1:**359–369.
26. **Mattaj, I. W., and L. Englmeier.** 1998. Nucleocytoplasmic transport: the soluble phase. Annu. Rev. Biochem. **67:**265–306.
27. **Melchior, F., and L. Gerace.** 1998. Two-way trafficking with Ran. Trends Cell Biol. **8:**175–179.
28. **Nakielny, S., S. Shaikh, B. Burke, and G. Dreyfuss.** 1999. Nup153 is an M9-containing mobile nucleoporin with a novel Ran-binding domain. EMBO J. **18:**1982–95.
29. **Ossareh-Nazari, B., F. Bachelerie, and C. Dargemont.** 1997. Evidence for a role of CRM1 in signal-mediated nuclear protein export. Science **278:**141–144.
30. **Pante, N., R. Bastos, I. McMorrow, B. Burke, and U. Aebi.** 1994. Interactions and three-dimensional localization of a group of nuclear pore complex proteins. J. Cell Biol. **126:**603–617.
31. **Pemberton, L. F., G. Blobel, and J. S. Rosenblum.** 1998. Transport routes through the nuclear pore complex. Curr. Opin. Cell Biol. **10:**392–399.
32. **Powers, M. A., D. J. Forbes, J. E. Dahlberg, and E. Lund.** 1997. The verte-

brate GLFG nucleoporin, Nup98, is an essential component of multiple RNA export pathways. J. Cell Biol. **136:**241–250.
33. **Radu, A., M. S. Moore, and G. Blobel.** 1995. The peptide repeat domain of nucleoporin Nup98 functions as a docking site in transport across the nuclear pore complex. Cell **81:**215–222.
34. **Ris, H.** 1991. The three-dimensional structure of the nuclear pore complex as seen by high-voltage microscopy and high-resolution low-voltage scanning electron microscopy. EMSA Bull. **21:**54–56.
35. **Shah, S., and D. J. Forbes.** 1998. Separate nuclear import pathways converge on the nucleoporin Nup153 and can be dissected with dominant-negative inhibitors. Curr. Biol. **8:**1376–1386.
36. **Shah, S., S. Tugendreich, and D. Forbes.** 1998. Major binding sites for the nuclear import receptor are the internal nucleoporin Nup153 and the adjacent nuclear filament protein. Tpr. J. Cell Biol. **141:**31–49.
36a. **Smitherman, M., K. Lee, R. Kapur, and B. E. Clurman.** 2000. Characterization and targeted disruption of murine Nup50, a $p27^{Kip1}$-interacting component of the nuclear pore complex. Mol. Cell. Biol. **20:**5631–5642.
37. **Snow, C. M., A. Senior, and L. Gerace.** 1987. Monoclonal antibodies identify a group of nuclear pore complex glycoproteins. J. Cell Biol. **104:**1143–1156.
38. **Stade, K., C. S. Ford, C. Guthrie, and K. Weis.** 1997. Exportin 1 (Crm1p) is an essential nuclear export factor. Cell **90:**1041–1050.
39. **Stoffler, D., B. Fahrenkrog, and U. Aebi.** 1999. The nuclear pore complex: from molecular architecture to functional dynamics. Curr. Opin. Cell Biol. **11:**391–401.
40. **Taniura, H., C. Glass, and L. Gerace.** 1995. A chromatin binding site in the tail domain of nuclear lamins that interacts with core histones. J. Cell Biol. **131:**33–44.
41. **Trichet, V., D. Shkolny, I. Dunham, D. Beare, and H. E. McDermid.** 1999. Mapping and complex expression pattern of the human NPAP60L nucleoporin gene. Cytogenet. Cell Genet. **85:**221–226.
42. **Ullman, K. S., S. Shah, M. A. Powers, and D. J. Forbes.** 1999. The nucleoporin nup153 plays a critical role in multiple types of nuclear export. Mol. Biol. Cell **10:**649–664.
43. **Wen, W., J. L. Meinkoth, R. Y. Tsien, and S. S. Taylor.** 1995. Identification of a signal for rapid export of proteins from the nucleus. Cell **82:**463–473.
44. **Wozniak, R. W., M. P. Rout, and J. D. Aitchison.** 1998. Karyopherins and kissing cousins. Trends Cell Biol. **8:**184–188.